VISUAL STUDIES OF WAKE STRUCTURE BEHIND TWO CYLINDERS IN TANDEM ARRANGEMENT

HUHE-AODE
Institute of Mechanics, Chinese Academy of Sciences : Research Associate

Tatsuno, Masakazu
Research Institute for Applied Mechanics, Kyushu University : Associate Professor

Taneda, Sadatoshi
Research Institute for Applied Mechanics, Kyushu University : Professor

https://doi.org/10.5109/6781018

出版情報：Reports of Research Institute for Applied Mechanics. 32 (99), pp.1-20, 1985-02. 九州大学応用力学研究所

Reports of Research Institute for Applied Mechanics
Vol. XXXII, No. 99, 1985

VISUAL STUDIES OF WAKE STRUCTURE BEHIND TWO CYLINDERS IN TANDEM ARRANGEMENT

By HUHE-AODE*, Masakazu TATSUNO† and Sadatoshi TANEDA‡

Wake structure behind two circular cylinders in tandem arrangement is investigated experimentally by means of a hot-wire anemometer and flow visualization techniques in the range of Reynolds number from 10^2 to 10^3. Spacing between central axes of two cylinders with equal diameter is varied in the range $1.5<s/d<10$, where s is the spacing and d the cylinder diameter. The downstream cylinder is stationary or forced to vibrate in the transverse direction at various frequencies and at two values of amplitudes of $0.1d$ and $0.3d$.

When both cylinders are stationary, the vortex shedding frequency measured behind the downstream cylinder changes discontinuously at a critical value of spacing for each Reynolds number. The flow visualization reveals that different patterns of vortex street appear in the wake according to spacings.

When the downstream cylinder is forced to vibrate sinusoidally at frequencies near the Strouhal frequency of vortex shedding for two stationary cylinders, the vortex shedding is synchronized with the vibrations of the cylinder. At two ends of the synchronization region, the elongation and contraction phenomena of vortex streets can be seen even at small oscillation amplitudes.

Key words: Two cylinders in tandem, Oscillations, Vortex street, Flow visualization

Nomenclature

d : cylinder diameter
U : velocity of main stream
s : separated spacing between centers of two cylinders
R_e : Reynolds number
f_c : oscillation frequency of downstream cylinder

* Research Associate, Institute of Mechanics, Chinese Academy of Sciences, Beijing.
† Associate Professor, Research Institute for Applied Mechanics, Kyushu University.
‡ Professor, Research Institute for Applied Mechanics, Kyushu University.

S_c : $f_c d/U$
a : oscillation amplitude of downstream cylinder
f_v : frequency of vortex shedding
S_v : Strouhal number, $f_v d/U$
L : longitudinal distance between successive vortices

1. Introduction

When a single cylinder performs transverse vibrations in a uniform flow, the vortex shedding is synchronized with the vibrations of the cylinder at frequencies near the Strouhal frequency of vortex shedding for the stationary cylinder[1)~7)].

On the other hand, wake interaction causes dramatic changes in the lift and drag acting on two cylinders in close proximity to each other, and most investigations dealing with this problem were reviewed by Zdravkovich[8)] for two stationary cylinders in various arrangements.

Now, when two cylinders are arranged in tandem and the downstream cylinder is vibrated transversely, the interaction between the vibrating cylinder and the wake flow has been investigated by several researchers[12)~15)]. For example, Tanida et al[13)]. measured the vortex shedding frequencies and the drag and lift forces acting on each cylinder for different separation gaps.

There are a number of relatively complex problems related to the mechanism of vortex formation. Then, further visual studies about vortex street structure behind two cylinders are practically and fundamentally important.

Present investigation is in two aspects;

(1) the study of the discontinuous changes in the vortex shedding frequencies,

(2) the study of effects of the Reynolds number, the separated spacing, the oscillation frequency of the cylinder and the amplitude of the cylinder on the vortex street structure around the synchronization region.

2. Experimental Apparatus and Methods

The experiments were carried out in a water tank 0.4 m wide, 0.4 m deep and 4 m long and equipped with a towing carriage, as shown in Fig. 1. The carriage speed was varied between 1.27 and 15 cm/sec in order to perform the experiments at $R_e = 10^2$, 3×10^2 and 10^3.

Two well polished brass circular cylinders with diameter of 1.0 cm and length of 30 cm were arranged in tandem. The upstream cylinder mounted vertically on the carriage was held stationary. The downstream cylinder was attached to the vibrating apparatus fixed on the car-

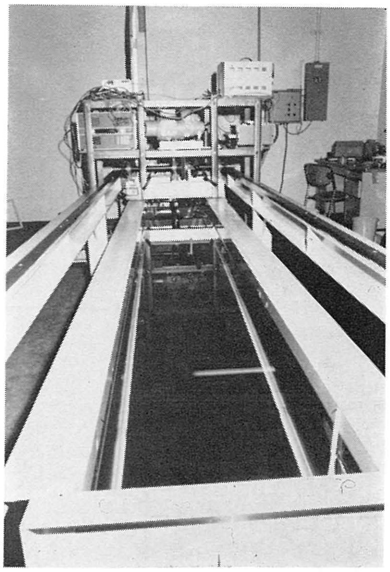

Fig. 1 Experimental apparatus.

riage. The amplitude of the oscillating cylinder was equal to 0.1 or 0.3 diameter length. The separating spacing between centers of two cylinders was varied in the range $1.5 < s/d < 10$. The vortex shedding frequencies were detected with a hot-wire anemometer located about 5 diameters apart from the downstream cylinder.

The vortex street was made visible by two kinds of electrolytic methods[16]. In the electrolytic precipitation method used for the flow at $R_e = 10^2$, the middle portions of the surfaces of test cylinders were coated with solder and a white colloidal cloud produced from solder electrochemically was used as a visual tracer. On the other hand, the hydrogen-bubble method was used to visualize the flow field at $R_e = 3 \times 10^2$. The tracer generating wire made of tungsten was placed ahead of the upstream cylinder. A slide projector was used in order to illuminate the horizontal thin plane of the flow field through the transparent side wall of the tank, and photographs of vortex street were taken with Nikon camera.

3. Experimental Results

3.1. Case of both cylinders at rest

The vortex shedding frequencies behind the downstream cylinder at $R_e = 10^2$, 3×10^2 and 10^3 are plotted in Fig. 2, together with other results[10,11,17,18]. The discontinuous change in values of Strouhal numbers

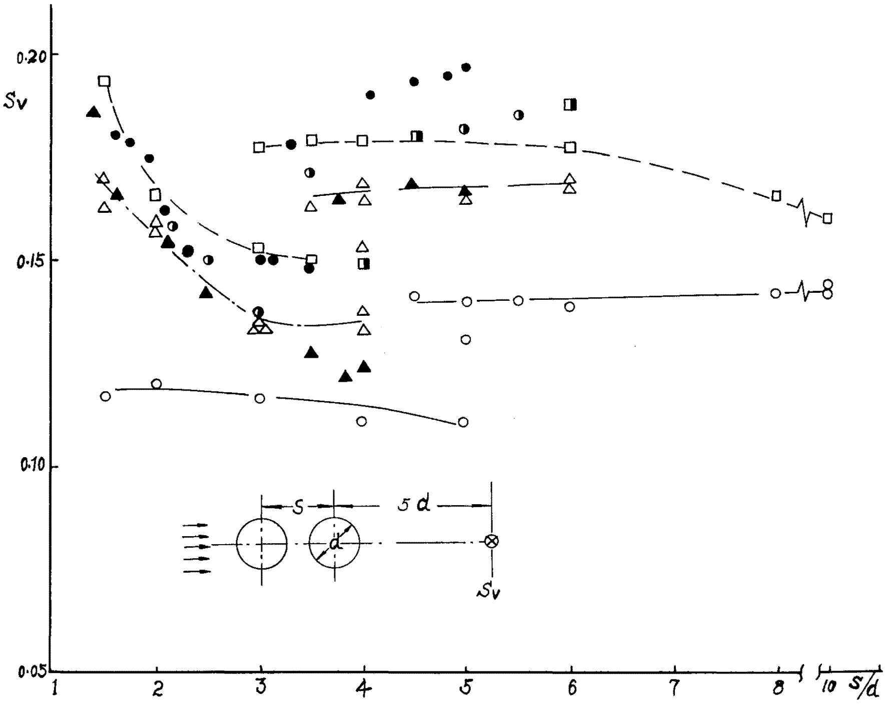

Fig. 2 Strouhal number of vortex shedding behind the downstream cylinder in tandem arrangement.
Present study: ○, $R_e=10^2$; △, $R_e=3\times10^2$; □, $R_e=10^3$, Igarashi: ●, $R_e=8.8\times10^3$, Ishigai et al.: ▲, $R_e=8.0\times10^3$, Kiya et al.: ◑, $R_e=1.58\times10^4$, Oka et al.: ◨, $R_e=8.8\times10^3$.

of vortex shedding appears in the range $4.5 < s/d < 5$ at $R_e=10^2$, $3.5 < s/d < 4.0$ at $R_e=3\times10^2$ and $3.0 < s/d < 3.5$ at $R_e=10^3$, respectively, as seen in Fig. 2. The value of critical spacing becomes small according as the Reynolds number grows large. Present results obtained at $R_e=10^3$ are supported by results of Kiya[10], Igarashi[11] and Oka[18]. Beyond the critical spacing, the Strouhal number approaches the value of a single cylinder as the spacing increases. In the case of $R_e=10^3$, however, the Strouhal number begins to decrease again beyond about 8 diameters spacing.

Figure 3 shows the changes in the flow pattern of vortex street with increasing the separated spacing at $R_e=10^2$. At values of spacing less than the critical one, twin recirculation regions are formed behind the downstream cylinder and the wake is in sinusoidal oscillations until about several diameters downstream. When $s/d=3.0$, the wake oscillates smoothly and the vortex street does not appear in the visible

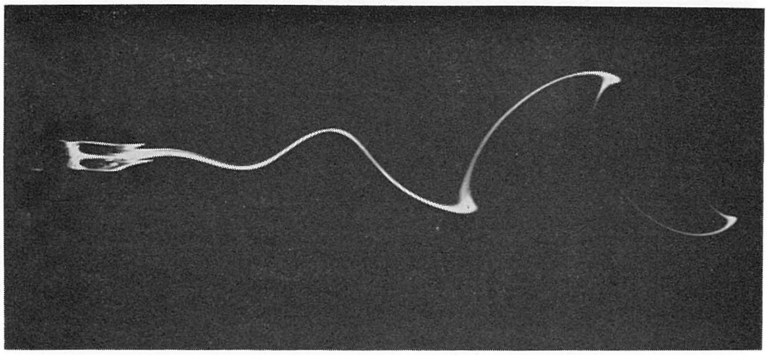

(a) $s/d=1.5$

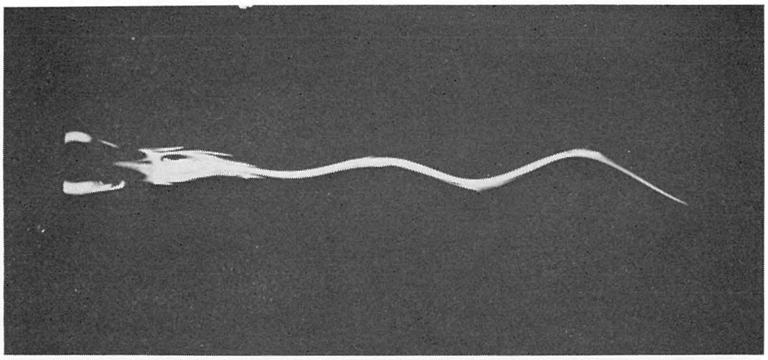

(b) $s/d=3.0$

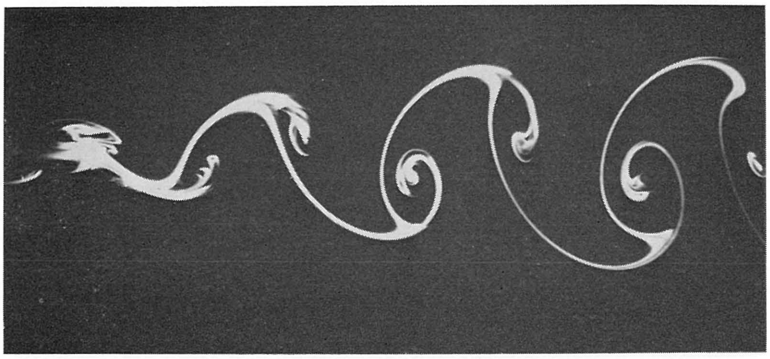

(c) $s/d=4.0$

Fig. 3 Vortex street behind two stationary cylinders at $R_e=10^2$.

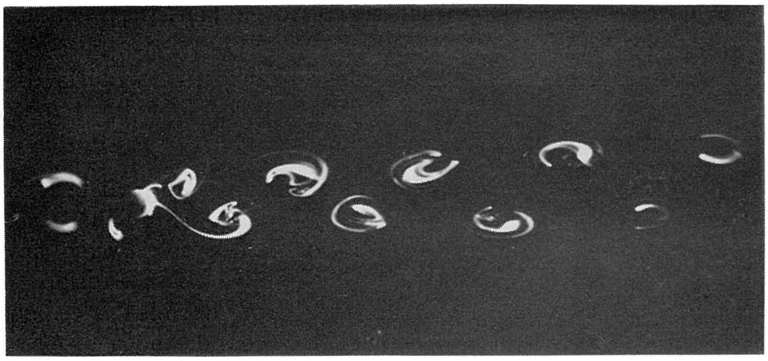

(d) $s/d=6.0$

Fig. 3 (continued)

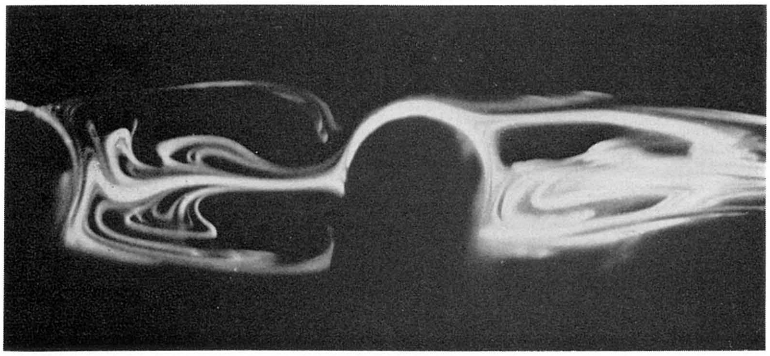

(a) $s/d=3.0$

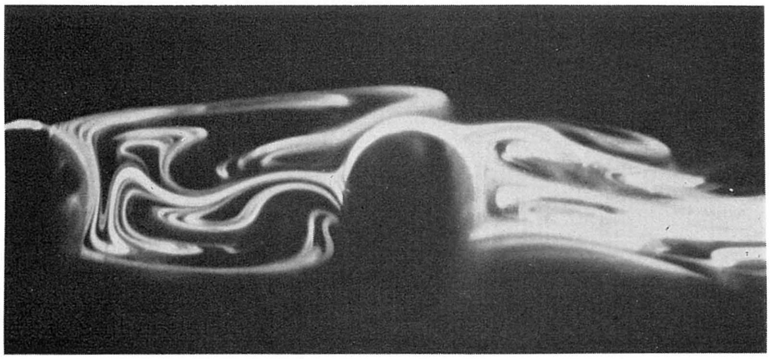

(b)-1 $s/d=3.0$

Fig. 4 Flow patterns in the gap between two cylinders at $R_e=10^2$.

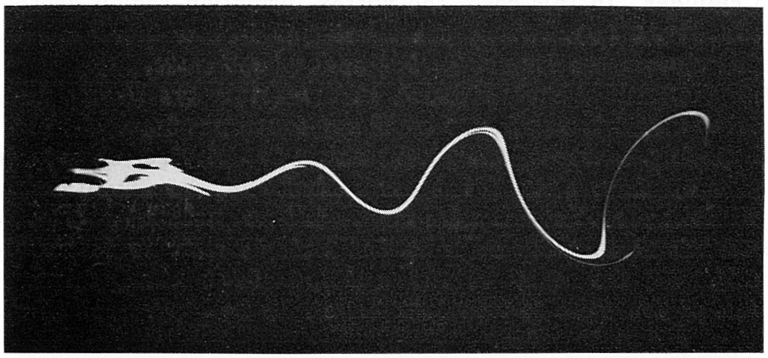

(b)-2 $s/d=3.0$

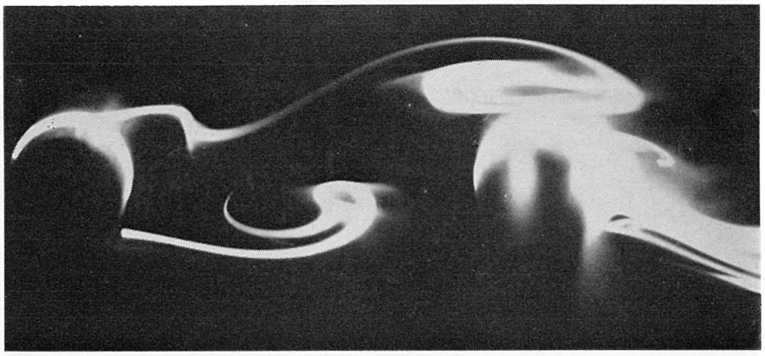

(c) $s/d=4.0$

Fig. 4 (continued).

part of the photograph, as seen in Fig. 3 (b). It indicates that the vortex formation region grows large with the spacing and is obviously longer than that for a single cylinder. This singular phenomenon may be explained through examining the flow pattern in the gap between the two cylinders, as shown in Fig. 4. Figure 4 (a) shows the flow pattern in the gap corresponding to the vortex street seen in Fig. 3(b). It will be seen from this figure that twin recirculations are formed in the gap and the flow which separates from the upstream cylinder does not reattach to the downstream cylinder. At the same separated spacing, however, another flow pattern was observed, as seen in Fig. 4 (b). In this case, the flows which separate from the right and left sides of the upstream cylinder reattach to the downstream cylinder alternately, and the vortex formation region behind the downstream cylinder decreases. At $s/d=4$, the flows separated from the upstream cylinder begin to roll up alternately, and then reattach to the downstream cylinder. In this case, the vortex formation region decreases in size (see Fig. 3 (c)). When the spacing is further increased, two full developed streets are formed behind each of cylinders.

Flow patterns of vortex street at $R_e=3\times10^2$ are shown in Fig. 5. The vortex street is regular at small separated spacings. At the upper critical spacing, however, the vortex street is distorted, as seen in Fig. 5 (d). At spacings over the upper critical one, the entire wake turns into turbulent vortex street with some distinct periodicity (Fig. 5 (e)). It is well known that the wake behind a single cylinder is turbulent at $R_e=3\times10^2$. In the case of two cylinders in tandem, however, the transition of the wake to turbulent flows may be suppressed at spacings below than a certain value.

3.2. Case of downstream cylinder oscillating transversely

The vortex shedding frequencies measured at $a/d=0.3$ and at two values of Reynolds numbers are plotted in Fig. 6. As be seen from

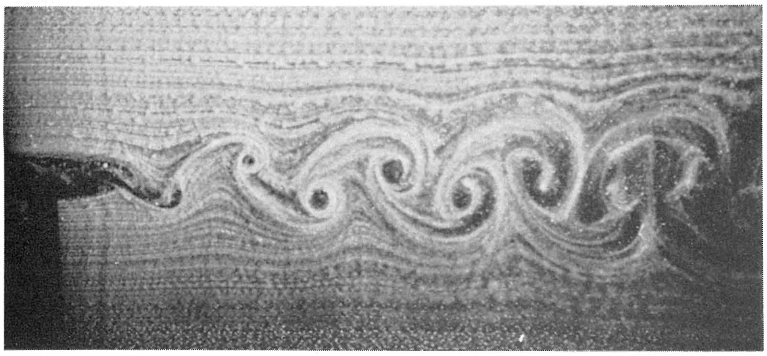

(a) $s/d=1.5$

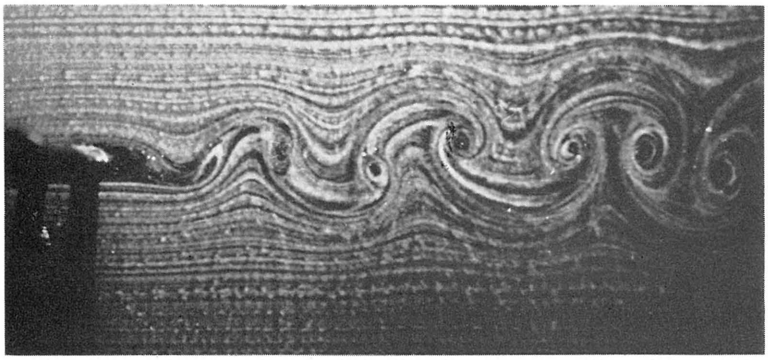

(b) $s/d=2.0$

Fig. 5 Vortex street behind two stationary cylinders at $R_e=3\times10^2$.

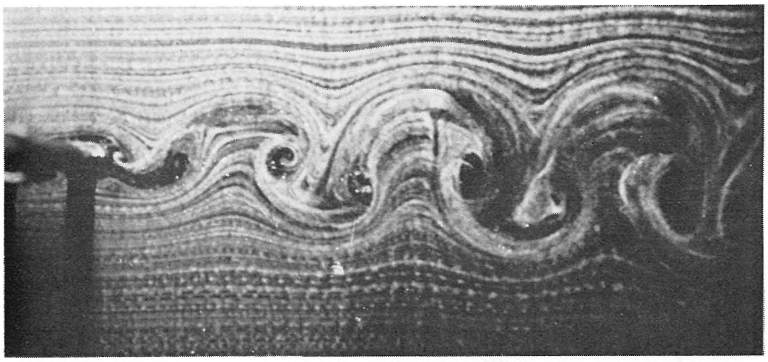

(c) $s/d=3.0$

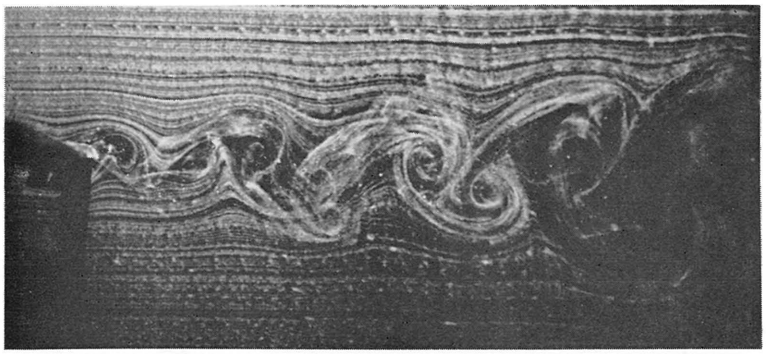

(d) $s/d=4.0$

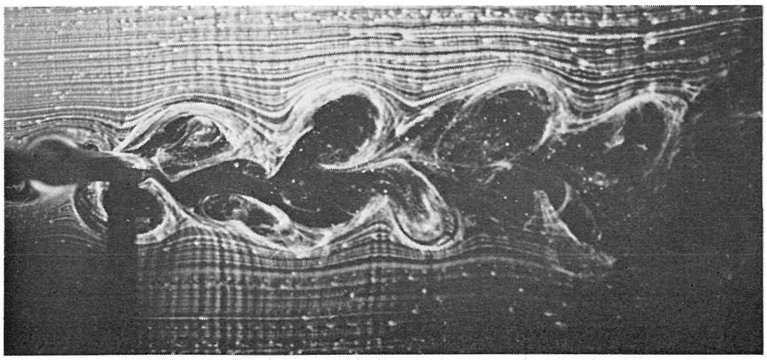

(e) $s/d=6.0$

Fig. 5 (continued).

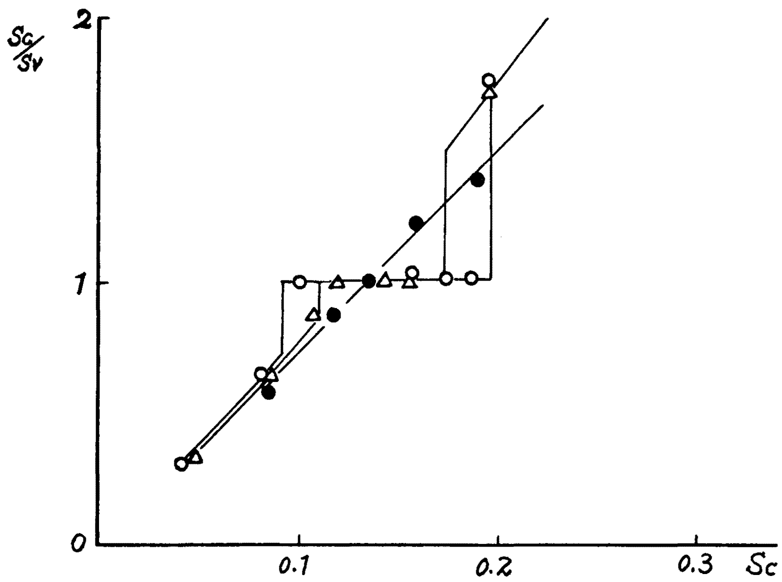

(a) $R_e = 10^2$: ○, $s/d = 1.5$; △, $s/d = 4.0$; ●, $s/d = 6.0$

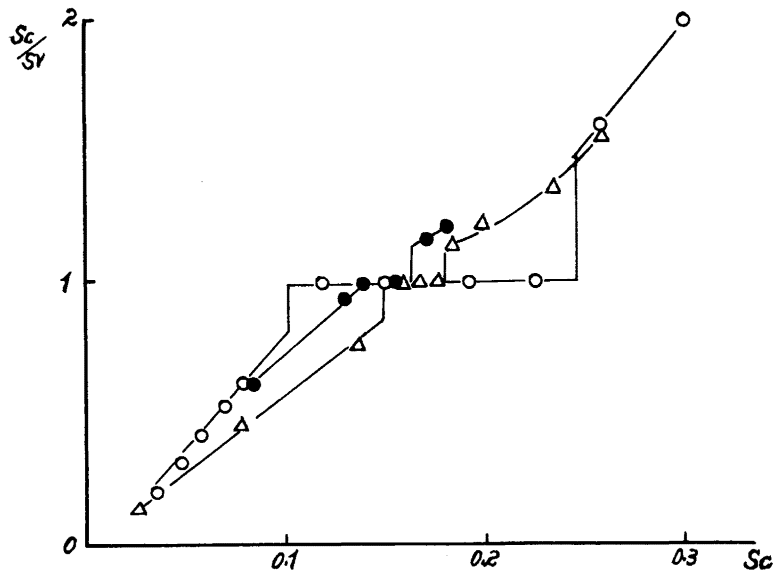

(b) $R_e = 10^3$: ○, $s/d = 1.5$; △, $s/d = 3.0$; ●, $s/d = 6.0$

Fig. 6 Ratio of cylinder oscillation and vortex shedding frequencies at $a/d = 0.3$.

this figure, the vortex shedding is synchronized with the vibrations of the cylinder at spacings smaller than a certain value. At $s/d=1.5$, the synchronization region extends over the range $0.09 < S_c < 0.2$ at $R_e=10^2$ and $0.1 < S_c < 0.25$ at $R_e=3\times10^2$ and 10^3, respectively. If the amplitude is decreased to $0.1d$, the synchronization region shrinks to the range $0.11 < S_c < 0.22$ at $R_e=3\times10^2$. It is evident that the synchronization region decreases as the spacing increases. When $R_e=10^2$, the synchronization disappears at $s/d=6$, but it can be still observed at $s/d=6$ for $R_e=10^3$. In view of the present result, the synchronization region becomes large with increasing the amplitude, with decreasing the spacing or with increasing the Reynolds number.

Figure 7 shows several photographs of the vortex street at $R_e=10^2$, $a/d=0.3$ and $s/d=1.5$. It shows that the vortex street is regular at small frequencies. When the oscillation frequency increases to the value corresponding to $S_c=0.076$, a pair of symmetric vortices are formed in the near wake, and the wake develops into an alternate vortex street in the downstream direction (Fig. 7 (b)). When the downstream cylinder is oscillated at the lower end frequency of the synchronization region, two vortices of same sign are formed successively in each half cycle of oscillations (Fig. 7 (c)). Subsequently, they coalesce into the alternate vortex street. In the synchronization region, the vortex street gets regular and the lateral spacing between two rows becomes narrower. At $S_c=0.19$, the upper end of the synchronization region, the vortex street, at first, is regular, but becomes unstable and the wake grows wider downstream. The flow pattern at high oscillation frequency of $S_c=0.38$ becomes to be similar to that at small frequency of $S_c=0.038$. At the same time, it is noted that the flow pattern in the gap between two cylinders in each case is similar to each other.

Figure 8 shows the vortex street at $R_e=3\times10^2$ and $a/d=0.3$. The pattern of vortex street is unstable and irregular at the frequency of the lower end of the synchronization region, as seen in Fig. 8 (b). In the synchronization region, the pattern of the vortex street is regular and maintained stable downstream. Furthermore, the ratio of the lateral spacing between two rows to the longitudinal distance between successive vortices in the same row becomes large as increasing the oscillation frequency. At the upper end of the synchronization region, the regular vortex street appears in the near wake, but it turns into irregular pattern in the downstream direction.

Figure 9 shows the vortex street at a large value of S_c, $a/d=0.3$ and $s/d=1.5$. In this case, the values of R_e and a/d are equal to that of Fig. 8, but the value of s/d is larger than that of Fig. 8. The vortex street shows a strange pattern. One counterclockwise, one clockwise and another small counterclockwise vortices are shed in every two cy-

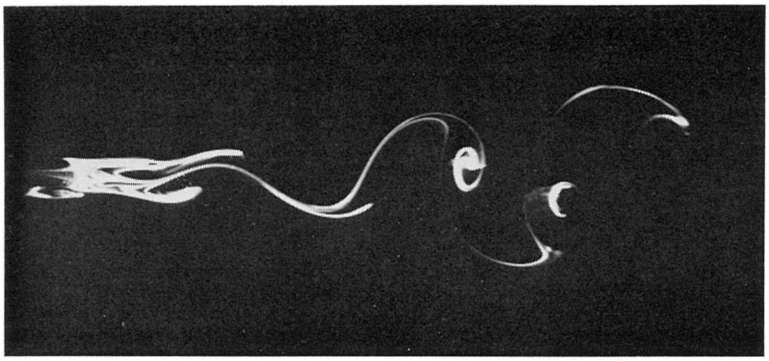

(a) $S_c=0.038$, $S_c/S_v=0.32$

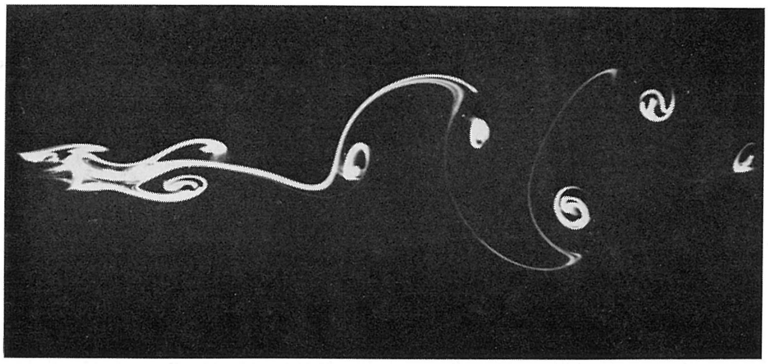

(b) $S_c=0.076$, $S_c/S_v=0.63$

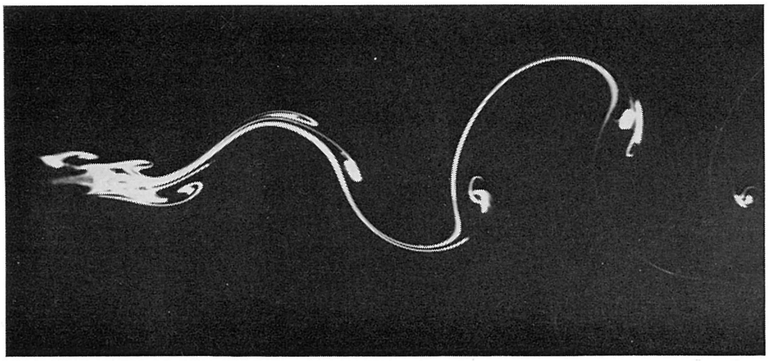

(c) $S_c=0.1$, $S_c/S_v=1.0$

Fig. 7 Changes in vortex street in the case of downstream cylinder oscillating at $R_e=10^2$, $a/d=0.3$ and $s/d=1.5$.

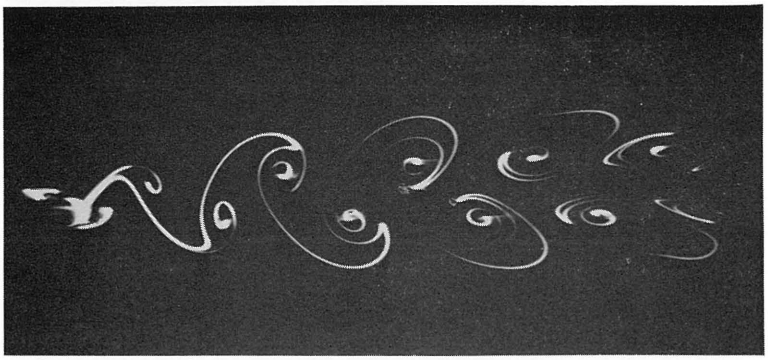

(d) $S_c=0.178$, $S_c/S_v=1.0$

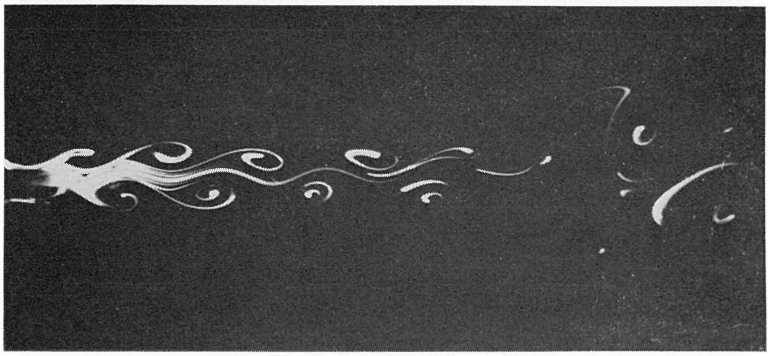

(e) $S_c=0.19$, $S_c/S_v=1.0$

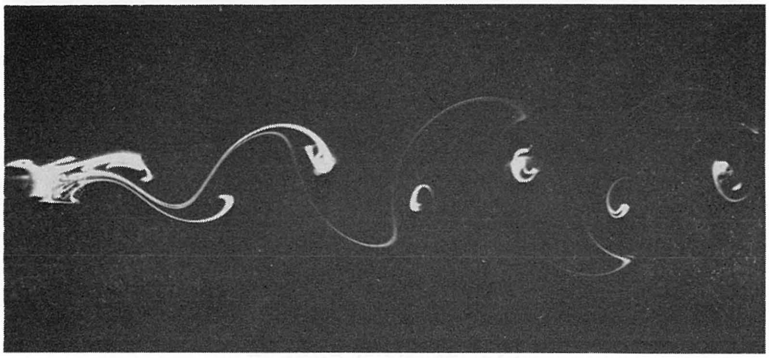

(f) $S_c=0.38$, $S_c/S_v=3.0$

Fig. 7 (continued).

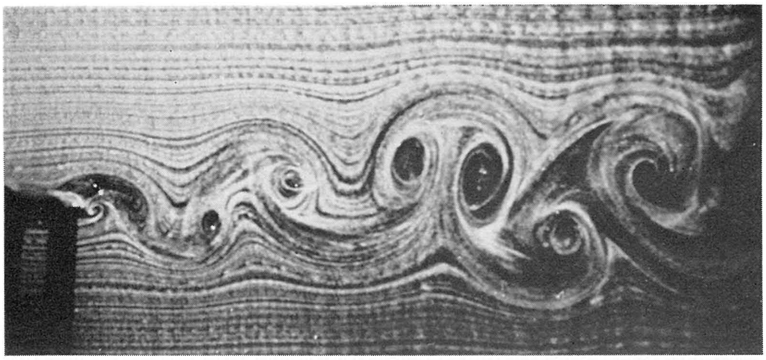

(a) $S_c=0.07$, $S_c/S_v=0.5$

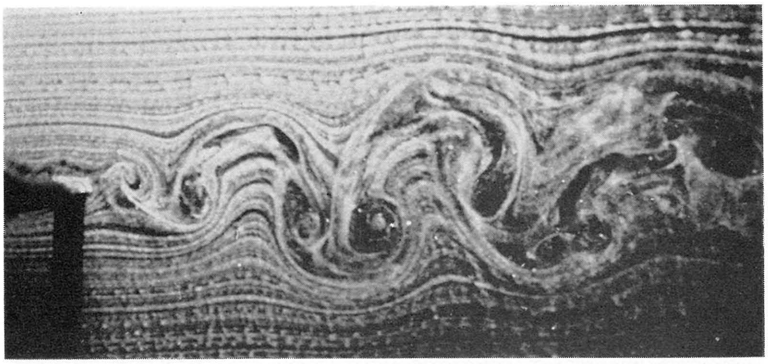

(b) $S_c=0.12$, $S_c/S_v=1.0$

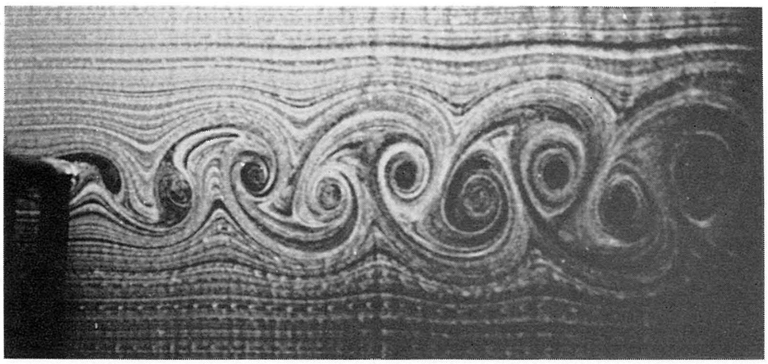

(c) $S_c=0.175$, $S_c/S_v=1.0$

Fig. 8 Changes in vortex street in the case of downstream cylinder oscillating at $R_e=3\times10^2$, $a/d=0.3$ and $s/d=1.0$.

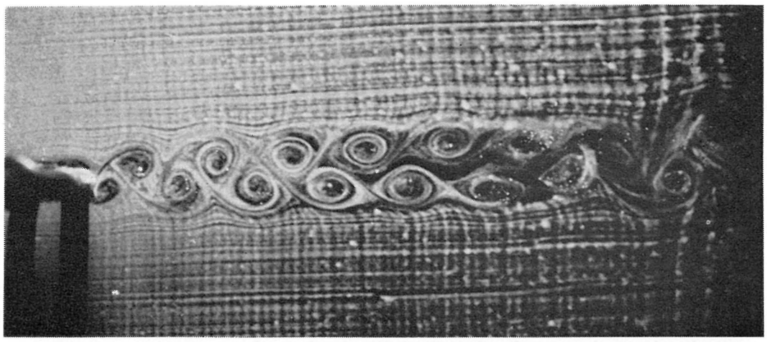

(d) $S_c=0.22$, $S_c/S_v=1.0$

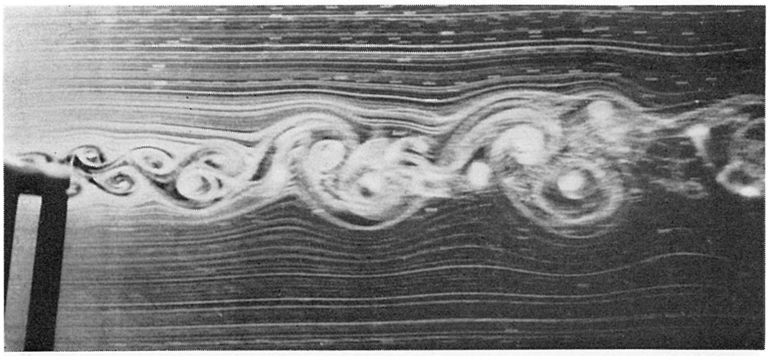

(e) $S_c=0.24$

Fig. 8 (continued).

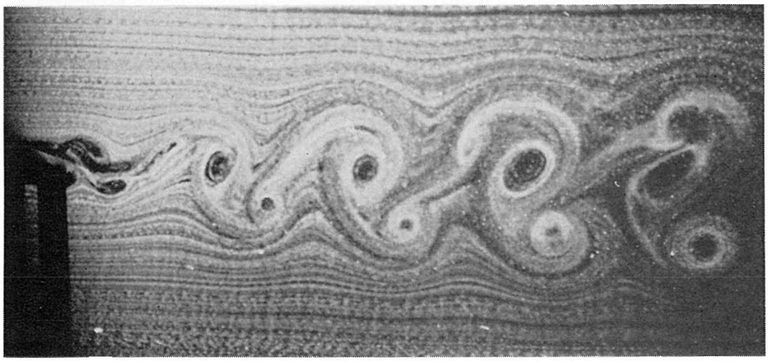

Fig. 9 Vortex street in the case of downstream cylinder oscillating at $R_e=3\times10^2$, $a/d=0.3$ and $s/d=1.5$.
$S_c=0.32$, $S_c/S_v=2.0$

cles of the cylinder oscillation, and these three vortices are arranged in a vertical line as they move downstream.

Several photographs of vortex streets are shown in Fig. 10 at small oscillation amplitude and $R_e=3\times10^2$. They show the similar changes in patterns to that at large amplitude.

The measured values of longitudinal vortex spacings are plotted against S_c at $R_e=10^2$ and 3×10^2 in Fig. 11. The vortex spacing becomes irregular and reaches the highest value at the lower end of the synchronization region. Subsequently, it decreases monotonically with the oscillation frequencies in the synchronization region, and reaches the minimum value at the upper end of that region. When the oscillation frequency is just beyond the upper end value of the synchronization region, the longitudinal vortex spacing discontinuously increases and then reaches a fixed value for each value of s/d and R_e. It is noted in Fig. 11 that the longitudinal vortex spacing at $R_e=3\times10^2$ is smaller

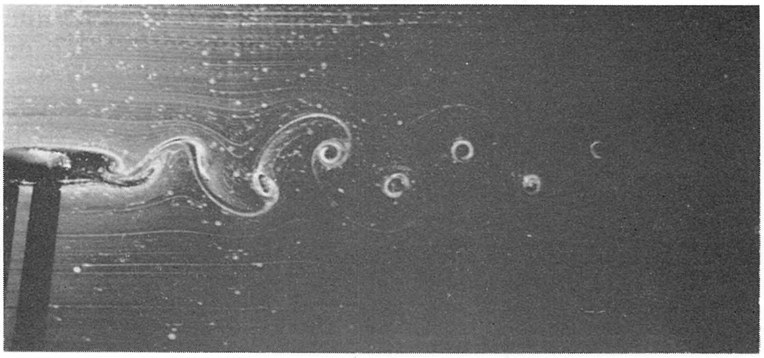

(a) $S_c=0$

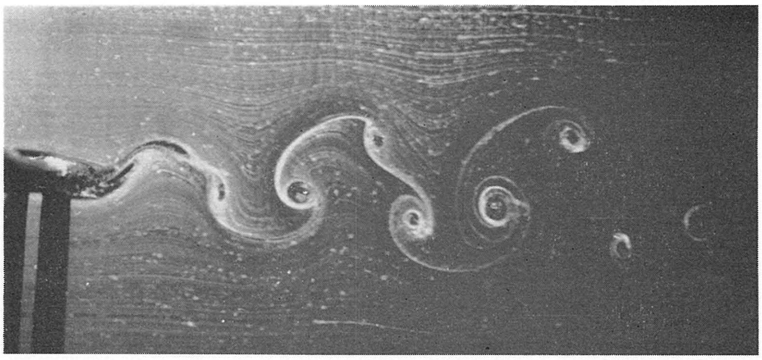

(b) $S_c=0.14$, $S_c/S_v=1.0$

Fig. 10 Changes in vortex street in the case of downstream cylinder oscillating at $R_e=3\times10^2$, $a/d=0.1$ and $s/d=1.5$.

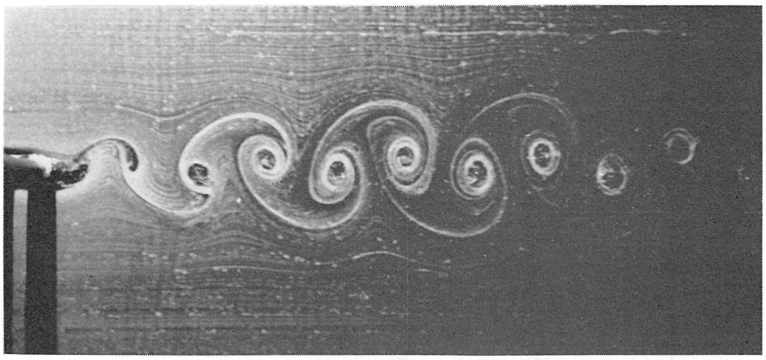

(c) $S_c=0.187$, $S_c/S_v=1.0$

(d) $S_c=0.25$, $S_c/S_v=1.0$

(e) $S_c=0.382$, $S_c/S_v=2.0$

Fig. 10 (continued).

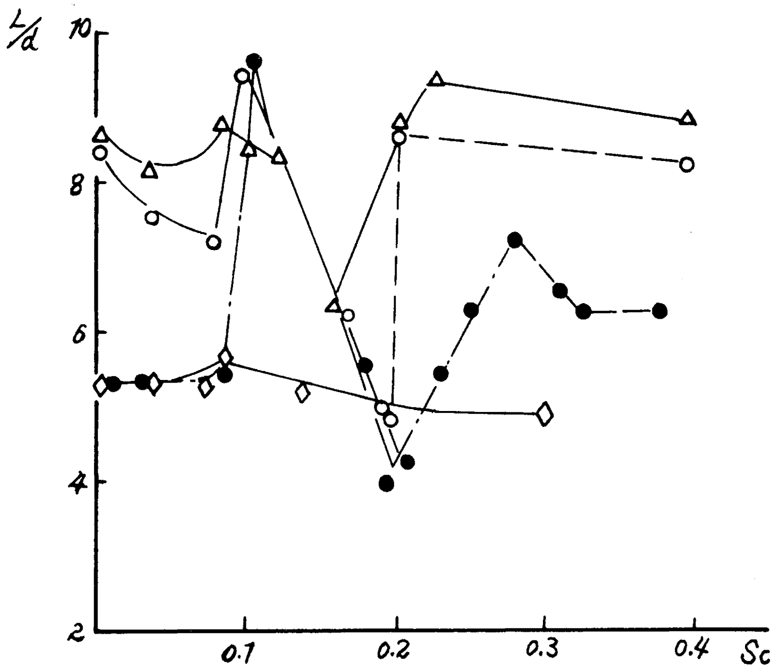

Fig. 11 Variation of the longitudinal vortex spacing in the case of downstream cylinder oscillating at $a/d=0.3$.
$R_e=10^2$: ○, $s/d=1.5$; △, $s/d=4.0$; ◇, $s/d=6.0$; $R_e=3\times10^2$: ●, $s/d=1.5$.

than that at $R_e=10^2$ except in the synchronization region where the vortex spacing is insensitive to the Reynolds number.

Figure 12 reveals that the oscillation amplitude does not affect greatly the longitudinal vortex spacing.

4. Conclusions

Experimental investigations of the vortex street behind two cylinders in tandem arrangement were carried out using the flow visualization techniques and the hot-wire anemometers.

(1) Case of both cylinders at rest

Discontinuous phenomena in vortex shedding frequencies appear in the range $4.5<s/d<5$ at $R_e=10^2$, $3.5<s/d<4.0$ at $R_e=3\times10^2$ and $3.0<s/d<3.5$ at $R_e=10^3$, respectively.

Vortex streets show different patterns at each value of s/d. Furthermore, the transition to turbulent wakes is suppressed in the case of two cylinders in tandem.

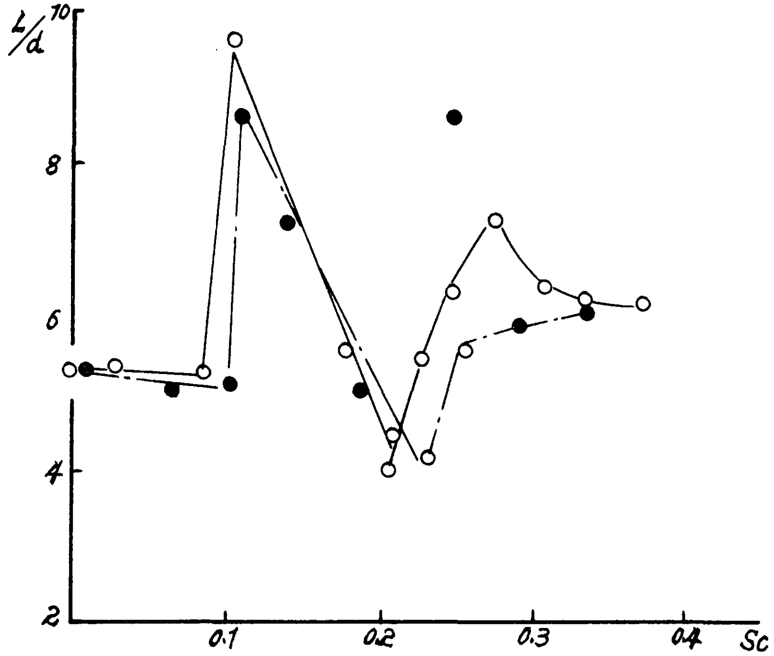

Fig. 12 Variation of the longitudinal vortex spacing in the case of downstream cylinder oscillating at $R_e=3\times10^2$.
●; $a/d=0.1$; ○, $a/d=0.3$.

(2) Case of downstream cylinder oscillating transversely

When the downstream cylinder performs sinusoidal oscillations at frequencies near the Strouhal frequency of vortex shedding for two stationary cylinders, the vortex shedding is synchronized with the cylinder oscillations. The synchronization region shrinks when the value of s/d increases or when a/d decreases. The patterns of vortex streets are regular in the synchronization region, but considerably irregular at both the lower and the upper ends of that region.

Acknowledgements

The authors would like to express their gratitude to Mr. K. Ishi-i for his assistance and Professor A. Okajima for his helpful discussions. One of the authors (Huhe-Aode) also wishes to thank Chinese Academy of Sciences, for making it possible for her to do research work in R. I. A. M., and to Japan Society for the Promotion of Science for their financial support.

References

1) Koopmann, G. H.: J. Fluid Mech. 28 (1967) 501.
2) Honji, H. and Taneda, S.: Rep. Res. Inst. Appl. Mech. **16**, No. 54 (1968) 211. Bull. Res. Inst. Appl. Mech. No. 30 (1968) 4.
3) Griffin, O. M.: Trans. ASME, J. Appl. Mech. 38 (1971) 729.
4) Griffin, O. M. and Votaw, C. W.: J. Fluid Mech. 55 (1972) 31.
5) Griffin, O. M.: Trans. ASME, J. Fluids Engng, 95 (1973) 579.
6) Griffin, O. M. and Ramberg, S. E.: J. Fluid Mech. 66 (1974) 553.
7) Zdravkovich, M. M.: Trans, ASME, J. Fluids Engng, 104 (1982) 513.
8) Zdravkovich, M. M.: Trans. ASME, J. Fluids Engng, 99 (1977) 618.
9) Okajima, A.: Bull. JSME, **22**, No. 166 (1979) 504.
10) Kiya, M., Arie, M., Tamura, H. and Mori, H.: Trans. ASME, J. Fluids Engng, 102 (1980) 166.
11) Igarashi, T.: Bull. JSME, **24**, No. 188 (1981) 323.
12) Zdravkovich, M. M.: *Flow-Induced Structural Vibration* (Ed. Naudascher, E., Springer, Berlin, 1974) 631.
13) Tanida, Y., Okajima, A. and Watanabe, Y.: J. Fluid Mech. 61 (1973) 769.
14) King, R. and Johns, D. J.: J. Sound Vib. **45**, No. 2 (1976) 259.
15) Zdravkovich, M. M.: Proc. Intern. Conf. Flow Induced Vib. Fluid Engng, 1982.
16) Taneda, S., Honji, H. and Tatsuno, M.: J. Phys. Soc. Japan **37**, No. 3 (1974) 784.
17) Ishigai, S., Nishikawa, E., Nishimura, K. and Cho, K.: Bull. JSME, 15 (1972) 949.
18) Oka, S., Kostic, Z. G. and Sikmanovic, S.: Intern. Seminar Recent Develop. Heat Exchangers, Trogir, Yugoslavia 1972.
19) Thomas, D. G. and Kraus, K. A.: J. Appl. Phys. **35**, 12 (1964) 3458.

(Received November 29, 1984)